Temperature Analysis for Optimizing the Configuration of the Linear Cell

Jongwook Choi*, Sungcho Kim, Jeong Soo Kim
School of Mechanical and Aerospace Engineering, College of Engineering, Sunchon National University, Suncheon, Jeonnam 540-742, Korea

The market demand of display devices is drastically increasing in the information technology age. The research on OLED (Organic Light Emitting Diodes) display with the luminescence in itself is being more paid attention than LCD (Liquid Crystal display) with the light source from the back. The vapor deposition process is most essential in manufacturing OLED display. The temperature distribution of the linear cell in this process is closely related to securing the uniformity of organic materials on the substrate. This work analyzed the temperature distribution depending on the intervals between the crucible and the heating band as well as on the amount of the heat flux from the heating band. Moreover, the roles of the water jacket and the configuration of the cover within the linear cell were examined through the temperature analysis for six configurations of the linear cell. Under the above temperature analysis, the variations in the intervals and the amount of the heat flux were considered to have an effect on building the uniform temperature distribution within the crucible. It is predicted that the water jacket and the adequate configuration of the cover will prevent the blowout and clogging phenomena, respectively. The results can be used as the fundamental data for designing the optimal linear cell.

Key Words : OLED (Organic Light Emitting Diodes), Vapor Deposition Process, Linear Cell, Temperature Analysis

1. Introduction

The research on the information devices has been being constantly conducted since the demand on them has been on the increase in the information technology era. Widely used in the past, CRT (Cathode Ray Tube) has been fading away due to a number of disadvantages in the aspect of weight, volume, flatness and resolution, comparing with FPD (Flat Panel Display). LCD (Liquid Crystal Display), one of FPDs, is being extensively spread these days owing to many advantages such as the thin thickness, the light weight, the low power consumption and so forth. Despite these strong points of LCD, the technology development of OLED display has been being largely researched as it is better than LCD in the brightness, the contrast, the view angle, the scale and so on (Tang et al., 1989 ; Kido et al., 1994 ; Hamada et al., 1995 ; Tokito et al., 1995 ; Granström and Inganäs, 1996). With the luminescence in itself, the wide view angle, the fast response and the low power consumption, OLED display has been focused as the next generation of display. It has already been adopted on the outside panel of mobile phones and will be expected to extend to the fields of PDA (Person Digital Assistants), digital camera, digital camcorder and even television monitor.

Since OLED was first recognized by Pope in 1963, investigations using the mono-molecule (Tang and VanSlyke, 1987) and the polymers (Burroughes et al., 1990) have been extensively performed.

* Corresponding Author,
E-mail : choijw99@sunchon.ac.kr
TEL : +82-61-750-3826; **FAX** : +82-61-750-3820
School of Mechanical and Aerospace Engineering, College of Engineering, Sunchon National University, Suncheon, Jeonnam 540-742, Korea. (Manuscript **Received** November 28, 2005; **Revised** March 31, 2006)

OLED display requires the technology for manufacturing thin films, which can be manufactured using the vapor deposition method in a vacuum state, suggested by Faraday in 1857. In this manufacturing process, the organic material in the crucible is sublimated and deposited on the substrate by heating in a vacuum condition. The evaporators for manufacturing OLED display can be classified as the point cell type and the linear cell type (Smith, 1994). While the crucible in the point cell takes on the small cylindrical configuration, the one in the linear cell does the long rectangular geometry. There is a disadvantage of being difficult to build the large-scaled display in the point cell, even though it can obtain the uniformity of the thin film with ease. On the other hand, a drawback of the linear cell lies in the difficulty of leading the uniformity of the thin film in spite of the benefit of being suitable in creating the large-scaled display. The uniformity of the thin film depends on the temperature distribution of the source, the organic material, in the crucible. That is because the source composed of particles is first sublimated from the place where it reaches out to the sublimation point in the crucible, and then deposited on the substrate. In brief, the temperature distribution in the source counts on the configuration of the linear cell. The studies concerning the acquisition of the uniform temperature distribution have been done in the point cell (Choi et al., 2004) and the linear cell (Choi et al., 2005). They proposed the ways of gaining the even temperature distribution, with the crucible configurations changed. In the previous study on the linear cell, the uniform temperature distribution was achieved after modifying the both ends of the crucible into the cylindrical configuration.

The present study intends to obtain the uniform temperature distribution, shifting the parameters such as the intervals between the crucible and the heating band, and the amount of the heat flux from the heating band. The geometry of the crucible remains unchanged in this work. Then, how the parameters can affect the temperature distribution is examined. Next, the temperature analysis is carried out on the six configurations with matching up the water jacket to the configurations of the cover in the linear cell. Then, how the water jacket and the configuration of the cover have an effect on the temperature distribution is inquired. The heat transfer by conduction and radiation is analyzed using STAR-CD (STAR-CD User Guide, 2004), a commercial code, and the grid system required in the temperature analysis is generated by ICEM CFD (ANSYS ICEM CFD User Manual, 2005).

2. Configurations and Computational Conditions

2.1 Parameters

The source heated in a vacuum state is deposited on the moving substrate in the linear cell as seen in Fig. 1. The general linear cell consists of the source, the crucible, and the upper and lower parts of the heating bands (Fig. 2). With the result of the temperature analysis in this linear cell, the deviation of the temperature occurred in the direction of the length of the source (Choi et al., 2005). In other words, the temperature value at both ends was marked higher than the one in the center of the source. It was noted that the source was hard to be evenly sublimated in such temperature distribution. Therefore, the temperature analysis should be conducted, so as to reduce the temperature deviation, based on the two occasions as suggested below. The calculation conditions are given in Fig. 2 and the dimensions of the configuration for the temperature analysis in Table 1. The escape boundary represents a non-reflecting surface at the outer boundary. The ini-

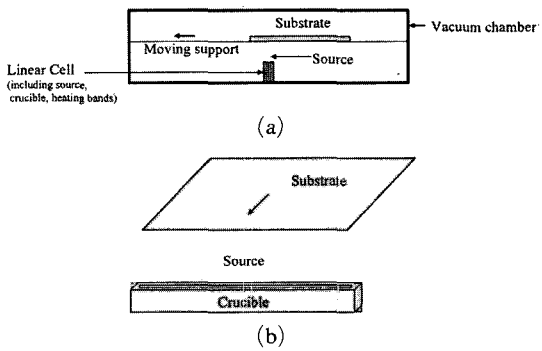

Fig. 1 Configuration of the linear cell

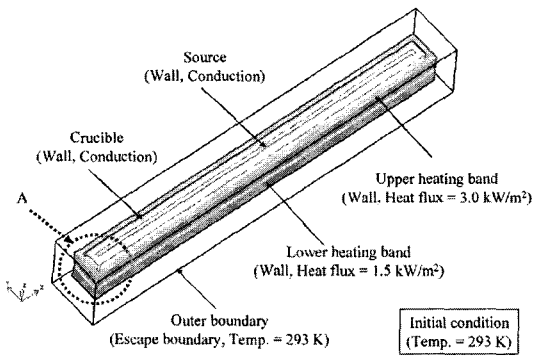

Fig. 2 General configuration and calculation conditions of the linear cell

Table 1 Dimensions of the linear cell

	Dimensions (mm)
Source	900×20×63
Crucible	910×30×95 (thickness : 10)
Heating band	950×70×40 (thickness : 10)
Outer boundary	1020×140×160

tial condition is set to 293K, the room temperature, and doesn't affect the final temperature distributions in the steady state.

2.1.1 Intervals between the crucible and the heating band

In general, the heat flux is more transferred into both ends of the crucible because of the characteristics of the configuration. Thus, a considerable amount of the sublimation takes place at both ends of the source, which makes the source not evenly deposited on the substrate. For this reason, the temperature deviation should be narrowed through controlling the intervals between both ends of the crucible and the heating band as in Fig. 3. The configurations on the linear cell are designed with an interval of 20, 60, 100, 140, and 200 mm, respectively. The interval of the general linear cell is 20 mm as seen in the dotted circle A in Fig. 2

2.1.2 Amount of the heat flux on the heating band

The heating bands as indicated in Fig. 4 are separated in order to obtain the uniform temperature distribution on the basis of the general linear cell. The amount of the heat flux is set, as given in Table 2, as 3.0, 4.0, 5.0, 5.5, and 6.0 kW/m^2 at both upper ends (U2) of the separated heating bands. These values are required for sublimating the source at the temperature of about 473K-573K. In Table 2, Flux_1 describes the calculation conditions of the unseparated heating

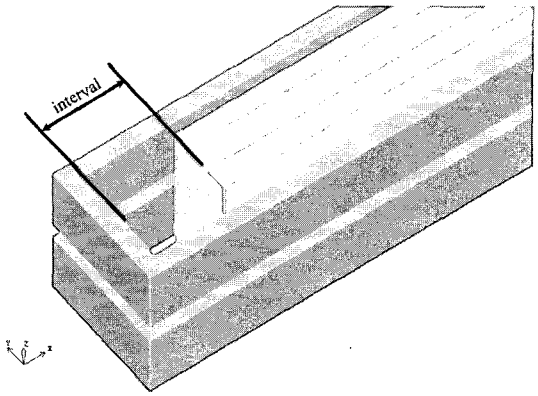

Fig. 3 Interval between the crucible and the heating band

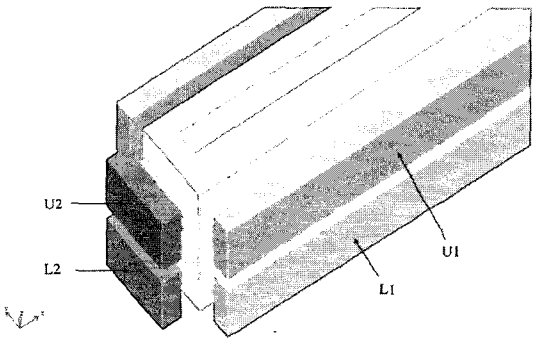

Fig. 4 Configuration of the separate heating bands

Table 2 Heat flux of the heating bands (kW/m^2)

Model No.	Upper heating bands		Lower heating bands	
	U1	**U2**	L1	L2
Flux_1	3.0		1.5	
Flux_2	30	**3.0**	1.5	1.5
Flux_3	30	**4.0**	1.5	1.5
Flux_4	30	**5.0**	1.5	1.5
Flux_5	30	**5.5**	1.5	1.5
Flux_6	30	**6.0**	1.5	1.5

bands in the general linear cell.

2.2 Six configurations

The water jacket and the cover are added to the linear cell in designing as in Fig. 5. Also, the heating bands are changed into the heating wires for the temperature analysis. The water jacket plays a role in preventing the lower part of source from reaching at the sublimated temperature by cooling it. The temperature of water jacket is set to 293K, which represents the room temperature in the vapor deposition process. The six configurations are indicated in Fig. 6. Geom_1, Geom_2 and Geom_3 contain the water jacket (marked by the dotted rectangles), while the rest of the cases are without it. The covers are categorized into three configurations, that is, Geom_1 and Geom_4 are one, Geom_2 and Geom_5 the other, and Geom_3 and Geom_6 another. The circles are added in the figures for the clear differences in the covers. The calculation conditions are described in Fig. 5.

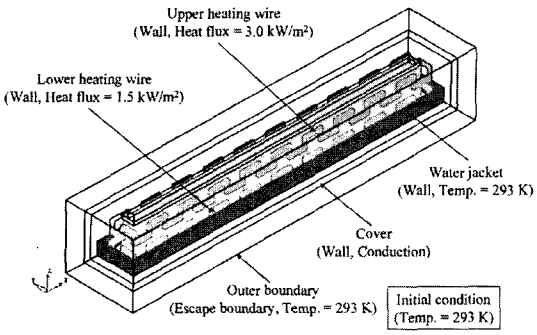

Fig. 5 Configuration of the linear cell with the water jacket and the cover

3. Temperature Analysis

The temperature distribution over the linear cell can be obtained by the analysis of the conductive heat transfer in the solid domain and the radiative heat transfer in the vacuum domain (fluid domain). The heat conduction equation used in the solid domain is given by Eq. (1).

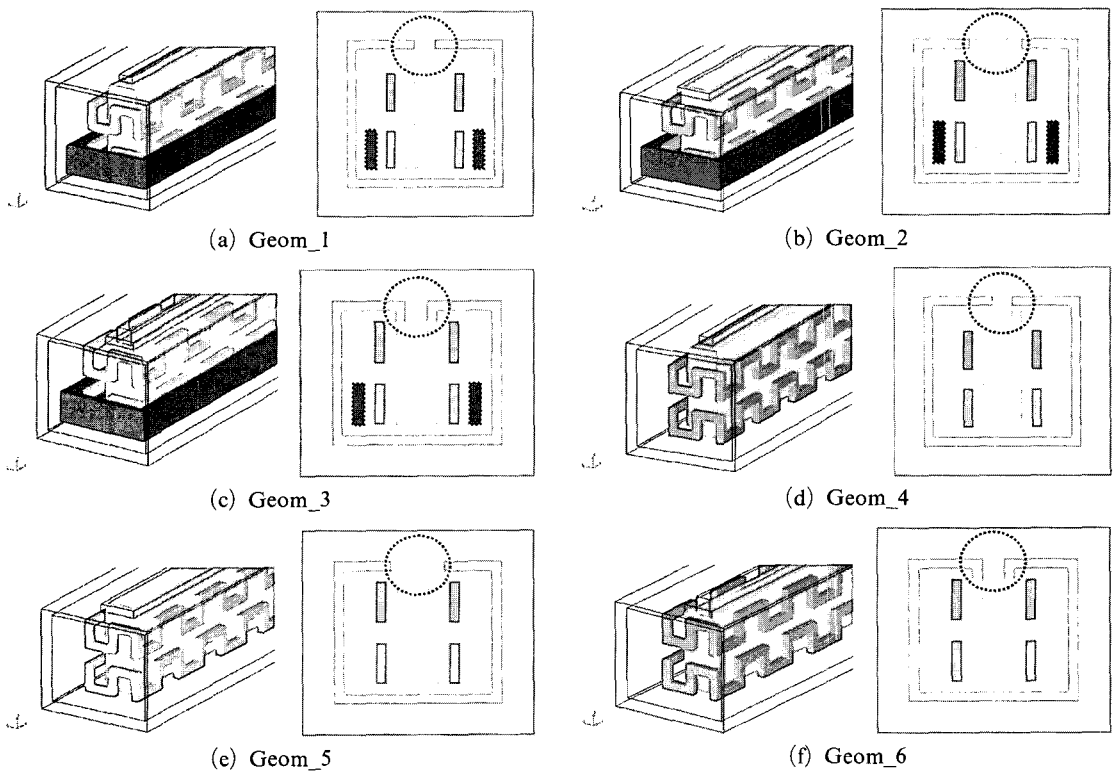

(a) Geom_1 (b) Geom_2

(c) Geom_3 (d) Geom_4

(e) Geom_5 (f) Geom_6

Fig. 6 The six configurations of the linear cell

$$\frac{\partial}{\partial x_j}\left(k\frac{\partial T}{\partial x_j}\right)+s_e=0 \tag{1}$$

where T refers to temperature and k conductivity of the solid material. As for s_e, it is the heat generation from radiation energy at the solid/fluid interface. The temperature distribution for the source and the crucible can be obtained in the similar way to the temperature analysis for compound materials with different properties. The numerical analysis over the vacuum domain is carried out by setting the flow velocity as 0 m/s and the conductivity as the lowest value (STAR-CD Tutorials, 2004). The properties of the materials are arranged in Table 3.

The DBM (Discrete Beam Method) is employed for computing the radiative heat transfer and the surfaces are assumed to be of the grey Lambert type. The surface boundaries are subdivided into patches, which the beams are individually emitted from. As the beams strike the opposite patches, the total radiation flux leaving the patch i is given by Eq. (2).

$$J_i=\varepsilon_r E_{B,i}+\rho_r I_i \tag{2}$$

where ε_r refers to emissivity, $E_{B,I}$ $(=\sigma T_i^4)$ blackbody emission flux, ρ_r reflectivity, and $I_i\left(=\sum_j F_{ji}J_i\right)$ incident flux, in which σ means Stefan-boltzmann constant and F_{ji} is given in Eq. (3). The emissivities of the crucible, the source, and the heating bands in the numerical analysis are set to 0.69, 0.5 and 0.19, respectively.

$$F_{ij}=\sum_{k=1}^{N_{L,i}}\alpha_k f_{ij} \tag{3}$$

where α_k is equal to 1 if the beam hits surface j or zero otherwise, and f_{ij} is the view factor for a single beam. The total number of beams, $N_{L,i}$ is $4N^2$, in which N is the number of subdivisions in one direction (STAR-CD Methodology, 2004).

Meanwhile, when the heat flux is prescribed at the boundary condition for the heating bands, the wall temperature (T_w) can be deduced by solving the non-linear polynomial as in Eq. (4).

$$q''_w=\alpha_r I_i-\varepsilon_r\sigma T_w^4-h_t(T_w-T_f)+q''_d \tag{4}$$

where q''_w is the total wall heat flux, h_t the local convective heat transfer coefficient, T_f the adjacent fluid temperature, q''_d the heat flux generated at internal conducting boundaries.

Table 3 Properties of the materials

Material	Density (kg/m^3)	Specific heat (J/kgK)	Conductivity (W/mK)
Fluid	1.205	1,006	1.0×10^{-7}
Solid (Crucible)	3,960	850	30
Solid (Source)	105	1,400	0.35

4. Results

4.1 Intervals between the crucible and the heating band

When the intervals between the crucible and the heating band are 20, 60, 100, 140 and 200 mm, respectively, the temperature variations toward the length at the edge of the upper source are plotted in Fig. 7. The position plotting the temperature variations is where the source is first sublimated. At this position, the even temperature distribution leads to the uniformity of thin film in the vapor deposition process because the amount of the sublimated source depends on the temperature. The non-dimensional temperature (θ) and the non-dimensional length (X) are given by Eq. (5)

$$\theta=(T-T_{\min})/(T_{\max}-T_{\min})$$
$$X=x/L \tag{5}$$

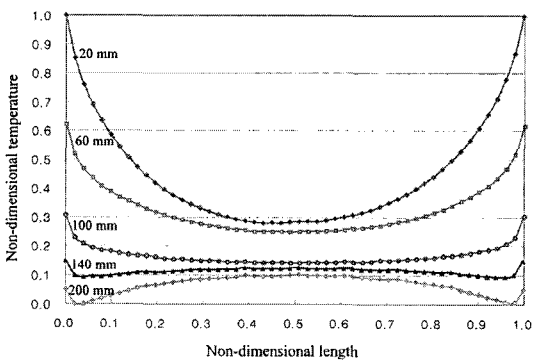

Fig. 7 Temperature variations with the intervals between the crucible and the heating band

where T refers to the temperature at the edge of the upper source shown in a dotted line in Fig. 8 (a), T_{min} the minimum value out of the temperature results of the varied intervals, T_{max} the maximum value out of the temperature results of the varied intervals, and L the length of the source. The temperature variation at an interval of 20 mm is shaped as a parabola with the highest temperature at both ends. Such temperature curve is owing to a large amount of the heat flux transmitted at both ends. A parabola pattern turns into almost the straight line as the interval is widened up to 140 mm.

When an interval of 140 mm is compared with an interval of 20 mm in the temperature distribution shown in Fig. 8, the former can be identified as the uniform temperature distribution in the direction of the length. This phenomenon is caused by increasing the intervals between the crucible and the heating band, resulting in the reduced amount of the heat flux at both ends. However, at an interval of 200 mm the temperature deviation in the direction of the length of the source become extended in the wake of lessening the amount of the heat flux acquired from both ends, which leads to the temperature drop. In consequence, it can be suggested that the reasonable interval between the crucible and the heating band plays a role in cutting down on the temperature deviation.

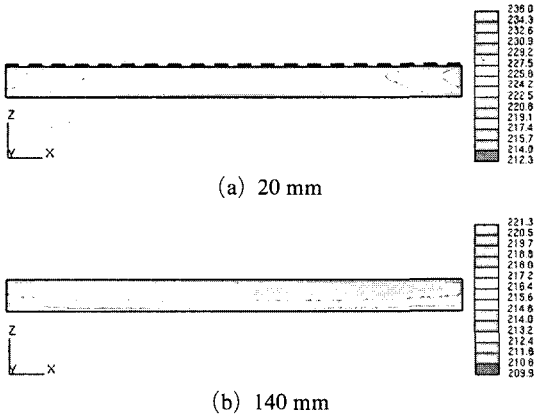

(a) 20 mm

(b) 140 mm

Fig. 8 Temperature distributions (℃) with the interval between the crucible and the heating band

4.2 Amount of the heat flux on the heating band

The temperature variations with the amount of the heat flux on the heating band are depicted in Fig. 9. In the case of Flux_1 with the unseparated heating bands, the temperature variation in the direction of the length at the edge of the upper source is a parabola in shape. Accordingly, by means of diminishing the temperature deviation between the both ends and the middle, both edges of the heating bands are made to separate (Fig. 4) and the amount of the heat flux in the upper part (U2) is set to 3.0, 4.0, 5.0, 5.5, and 6.0 kW/m^2, respectively. In the case of Flux_2, the relatively lower temperature value comes out at both ends against the one in the middle. That is because the amount of the heat flux declines due to the gaps

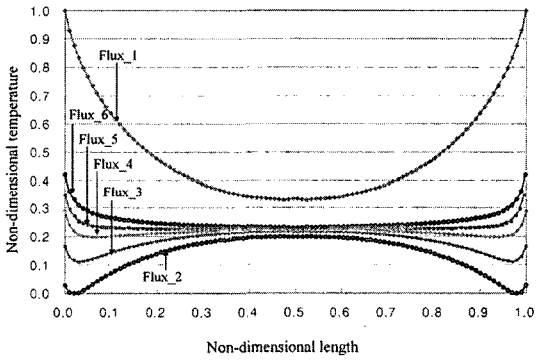

Fig. 9 Temperature variations with the amount of the heat flux in the separate heating bands

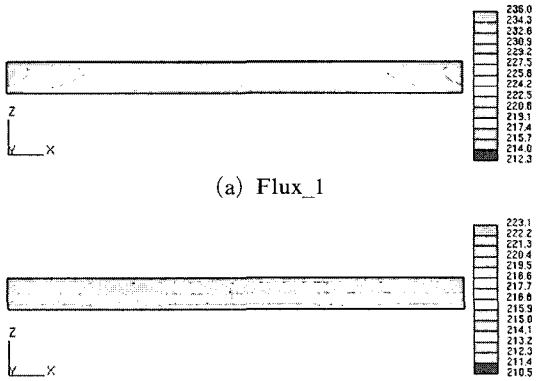

(a) Flux_1

(b) Flux_5

Fig. 10 Temperature distributions (℃) with the heat flux in the separate heating bands

generated by the detachment of the heating bands at both ends (L2, U2) from the ones in the direction of the length (L1, U1). It is mentioned that as the amount of the heat flux at both ends (U2) is getting increased, the temperature deviation is getting decreased in the cases of Flux_2 through Flux_6. In the case of Flux_5, about 90 % of the length, excluding both edges, keeps the almost uniform temperature distribution. Fig. 10 accounts for the results of comparing the temperature distributions toward the length in the cases of Flux_1 and Flux_5. Consequently, if the amount of the heat flux is adequately controlled at both ends through separating the heating bands, the temperature deviation toward the length of the source can be reduced.

4.3 Six configurations

The results of the temperature analysis on the six configurations are demonstrated in Fig. 11. A horizontal axis indicates the non-dimensional height of the source and a vertical axis points out the non-dimensional temperature of it. The temperature in the lower part of the source is shown lower than in the upper part in the cases of Geom_1, Geom_2 and Geom_4. On the contrary, if the temperature in the lower part of the source is higher than in the upper part, the vapor deposition process can not be implemented any longer on account of the blowout phenomenon. The blowout is that the source inside is sublimated and ruptured earlier than the upper part of the source. As the temperature distribution in the cases of Geom_1 and Geom_2 is relatively low in the lower part of the source under the influence of the water jacket, the blowout phenomenon does not occur. In the cases of Geom_3, Geom_5, and Geom_6, however, the blowout phenomenon is expected to appear because the temperature in the lower part marks the highest. Especially, in spite of the effect of the water jacket in the case of Geom_3, the blowout phenomenon is predicted under the influence of the configuration of the cover as shown in Fig. 6(c).

The temperature distributions in the cross section of the source, the crucible and the cover are given in Fig. 12. In the case of Geom_1, the temperature in the upper part of cover is lower than in the source as in Fig. 12(a). This fact leads to the clogging phenomenon that the sublimated source is deposited onto the cover with a relatively low temperature and the entry of the cover is blocked by the deposited source. This clogging phenomenon can be prohibited in the vapor deposition process by locating the cover in the outside of the crucible. The temperature distribution in the case of Geom_2 that the cover does

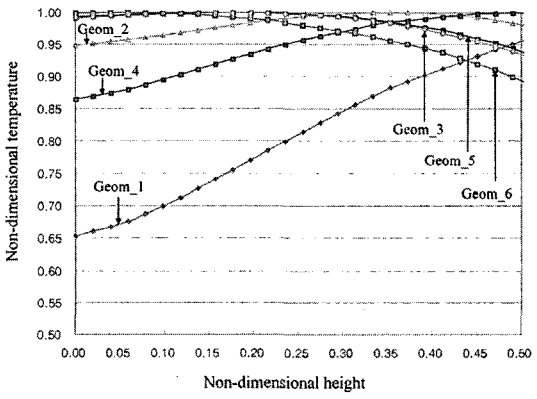

Fig. 11 Temperature variations with the configuration of the linear cell

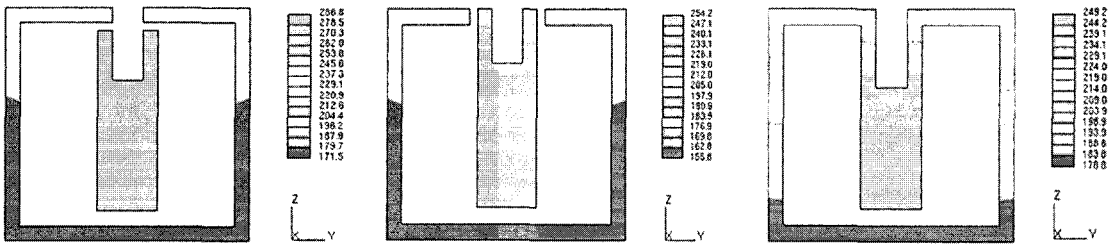

(a) Geom_1 (b) Geom_2 (c) Geom_3

Fig. 12 Temperature distributions (℃) with the configuration of the linear cell

not overlay on the crucible is presented as in Fig. 12(b). This configuration can keep the clogging phenomenon from occurring in the case of Geom_1. The temperature distribution in the case of Geom_3 with the configuration attached the crucible to the cover is shown in Fig. 12(c). In such case, since the temperature in the upper part of the cover is lower than in the source, as in the case of Geom_1, the clogging phenomenon is expected to emerge.

5. Conclusions

The most significant factor in the vapor deposition process using the linear cell is that the source is uniformly deposited onto the substrate. The temperature deviation in the direction of the length should be small for the purpose of the uniformity of the deposited source. However, the general linear cell takes on a parabola shape in the temperature distribution since getting a relatively considerable amount of the heat flux at both ends of the source. This research conducted the temperature analysis in the two ways so as to cut down on such temperature deviation. As a consequence, the temperature deviation could be narrowed through the first way, adjusting the intervals between the crucible and the heating band at both ends, in comparison with the general configuration. In addition, the uniform temperature distribution could be obtained through altering the amount of the heat flux in the upper part of the heating bands by separating the heating bands from both ends, the second way. These ways are likely to be applied when the linear cell is designed for the vapor deposition process with the uniformity. On the other hand, the temperature analysis on the six configurations was carried out with modifying the configurations of the general linear cell. With that result, the blowout phenomenon will be able to be prevented by putting the water jacket and the clogging phenomenon will be forbidden when the cover is not placed above the crucible or contacted to the crucible. All those results concerning the temperature analysis are supposed to be used as the ways of optimizing the design of the linear cell. The future work will be arranged to analyze taking the more realistic configurations into consideration to obtain the uniform temperature profile.

Acknowledgments

This work was supported by the Korea Research Foundation Grant funded by the Korean Government (MOEHRD) (R08-2003-000-10487-0).

References

ANSYS ICEM CFD/AI Environment 10.0 User Manual*, 2005, ANSYS Inc..

Burroughes, J. H., Bradley, D. D. C., Brown, A. R., Marks, R. N., Maackay, K., Friend, R. H., Burns, P. L. and Holmes, A. B., 1990, "Light-Emitting Diodes based on Conjugated Polymers," *Nature*, Vol. 347, pp. 539~541.

Choi, J. W., Kim, S. C. and Jung, H., 2004, "Temperature Analysis for the Point-Cell Source in the Vapor Deposition Process," *KSME International Journal*, Vol. 18, No. 9, pp. 1680~1688.

Choi, J. W., Kim, S. C. and Kim, J. S., 2005, "Temperature Analysis for the Linear Cell in the Vapor Deposition Process," *Journal of Mechanical Science and Technology*, Vol. 19, No. 6, pp. 1329~1337.

Granström, M. and Inganäs, 1996, "White Light Emission from a Polymer Blend Emitting Diode," *Applied Physics Letter*, Vol. 68, No. 2, pp. 147~149.

Hamada, Y., Sano, T., Shibata, K. and Kuroki, K., 1995, "Influence of the Emission Site on the Running Durability of Organic Electroluminescent Devices," *Japanese Journal of Applied Physics*, Vol. 34, pp. L824~L826.

Kido, J., Hongawa, K., Okuyama, K. and Nagai, K., 1994, "White Light-Emitting Organic Electroluminescent Devices using the Poly (N-Vinylcarbazole) Emitter Layer doped with Three Fluorescent Dyes," *Applied Physics Letters*, Vol. 64, No. 7, pp. 815~817.

STAR-CD Methodology (version 3.24), 2004, CD adapco Group, Chap. 9.

STAR-CD Tutorials (version 3.24), 2004, CD

adapco Group, Tutorial 12.

STAR-CD User Guide (version 3.24), 2004, CD adapco Group.

Smith, D. L., 1994, *Thin-Film Deposition Principles and Practice*, McGraw-Hill, pp. 63~118.

Tang, C. W. and VanSlyke, S. A., 1987, "Organic Electroluminescent Diodes," *Applied Physics Letter*, Vol. 51, No. 12, pp. 913~915.

Tang, C. W., VanSlyke, S. A. and Chen, C. H., 1989, "Electroluminescence of Doped Organic Thin Films," *Journal of Applied Physics*, Vol. 65, No. 9, pp. 3610~3616.

Tokito, S., Takata, J. and Taga, Y., 1995, "Organic/Inorganic Superlattices with Ordered Organic Layers," *Journal of Applied Physics*, Vol. 77, No. 5, pp. 1985~1989.